

## Mechanism of catalyst diffusion on magnesium oxide nanowire growth

Takeshi Yanagida,<sup>a)</sup> Kazuki Nagashima, Hidekazu Tanaka, and Tomoji Kawai  
*Institute of Scientific and Industrial Research, Osaka University, 8-1 Mihogaoka, Ibaraki,  
 Osaka 567-0047, Japan*

(Received 23 May 2007; accepted 12 July 2007; published online 6 August 2007)

In nanowire growth using vapor-liquid-solid (VLS) mechanism, controlling catalyst diffusion has been a key issue since VLS growth is essentially no longer feasible in the absence of catalyst on the tip. Here the authors demonstrate the controllability of catalyst diffusion on MgO nanowire growth by ambient pressure and discuss the underlying physical mechanism. Drastic enhancement of oxide nanowire growth was found when increasing the ambient pressure under oxygen atmosphere, and surprisingly even under argon atmosphere. This indicates that the ambient pressure rather than the amount of ambient oxygen dominates the oxide nanowire growth via suppressing the catalyst diffusion. © 2007 American Institute of Physics. [DOI: 10.1063/1.2768202]

Recently one-dimensional inorganic nanostructures formed using the vapor-liquid-solid (VLS) mechanism have attracted much attention.<sup>1</sup> Although the VLS in Si whisker growth was demonstrated more than 40 years ago,<sup>2,3</sup> a comprehensive understanding of the key factors affecting the VLS nanowire growth is still lacking. In fact investigations as to the VLS mechanism have been intensively reported recently, and the major interests have been directed at Si and compound semiconductors.<sup>4-7</sup> To expand the applicability of nanowires, it would be an interesting and challenging issue to incorporate more functionality of materials including metal oxides into the nanowires. The VLS mechanism for Si nanowire growth with Au catalyst is still complex, although the mechanism has been most intensively investigated.<sup>7</sup> An oxide nanowire growth mechanism is much more complicated and far from a comprehensive understanding.<sup>8-11</sup> Although it is important to fabricate well-defined long oxide nanowires in developing nanowire applications,<sup>4,7</sup> the lack of understanding the underlying mechanism has held back the arbitrary controllability of oxide nanowire morphologies.<sup>8-11</sup> Very recently it was discovered that the presence of ambient oxygen during Si nanowire growth allows fabricating long and untapered nanowires via reducing the diffusion of Au catalyst away from the droplet.<sup>7</sup> This discovery is a significant progress for fabricating well-defined inorganic nanowires; however, whether the same scenario is applicable to other nanowire growths has not been clarified. The role of such ambient oxygen on oxide nanowire growth essentially differs from that on Si nanowire growth due to the oxygen incorporation into the oxide nanowires. In addition, it is well known that the oxygen stoichiometry within oxides plays a crucial role on the properties.<sup>12,13</sup> Although several investigations on ZnO nanowires reported the ambient pressure dependence on the wire density,<sup>8,9</sup> the degree of Mg doping,<sup>10</sup> and the morphology variation,<sup>11</sup> understanding the underlying mechanism of the ambient pressure effect on the oxide nanowire growth is still scarce. As such investigating the role of the ambient oxygen on oxide nanowire growth is important not only for a fundamental understanding of complex oxide nanowire growth but also for fabricating advanced and well-defined functional oxide nanowires.

MgO has been used as a versatile single crystal substrate for various oxide film growths due to the small lattice mismatch with various transition metal oxides including ferroelectric, ferromagnet, and superconductor.<sup>14-16</sup> The feasibility of MgO nanowires has been proved to be powerful to integrate such rich functionalities of transition metal oxides into the oxide nanowires via the heterostructures.<sup>17,18</sup> Thus the controllability of MgO nanowire morphologies would pursue further integrations of functionalities of various metal oxides using such "oxide nanowire substrate." Previously we have reported the epitaxial growth of MgO nanowires,<sup>19</sup> the ambient temperature effect,<sup>20</sup> and the ablated particle flux effect<sup>21</sup> on MgO nanowire growth. However, the influence of ambient pressure has not been clarified yet. In this letter, we demonstrate the significant enhancement of MgO nanowire growth by controlling the ambient pressure under oxygen and/or argon atmospheres.

MgO nanowires were grown on MgO (100) single crystal substrate by Au catalyst-assisted pulsed laser deposition (PLD) technique.<sup>19-21</sup> Prior to the nanowire growth, Au catalysts were sputtered and patterned on the 5 × 5 mm<sup>2</sup> MgO single crystal substrate with a metal mask. The thickness of the sputtered Au is ~1 nm. The background pressure of the PLD chamber was set to be 10<sup>-4</sup> Pa. ArF excimer laser (Lamda-Physik, COMPex 102, λ = 193 nm) operating at the pulse repetition rate of 10 Hz and the laser energy of 40 mJ was used for the laser ablation. MgO single crystal was used for the source of Mg species vapor during the nanowire growth. The substrate was located at 30 mm away from the single crystal target. Oxygen gas (99.9999% purity) and/or argon gas (99.999% purity) were introduced into the chamber with controlling the ambient pressure. The ambient pressure was varied from 10<sup>-2</sup> to 10 Pa and kept constant during depositions. Prior to the laser ablation, the Au-coated MgO (100) substrate was preheated at 820 °C and kept for 10 min. After the deposition, the samples were cooled down to room temperature for 30 min. The nanowire morphology was characterized by field emission scanning electron microscopy (FESEM) (JEOL JSM-6330FT) at the accelerating voltage of 30 kV. The length of MgO nanowires was analyzed by averaging the data for 500 samples in FESEM images for statistical reliability. High-resolution transmission electron microscopy (HRTEM) (JEM-3000F) coupled with energy dispersive spectroscopy (EDS) was used to evaluate the di-

<sup>a)</sup>Electronic mail: yanagi32@sanken.osaka-u.ac.jp

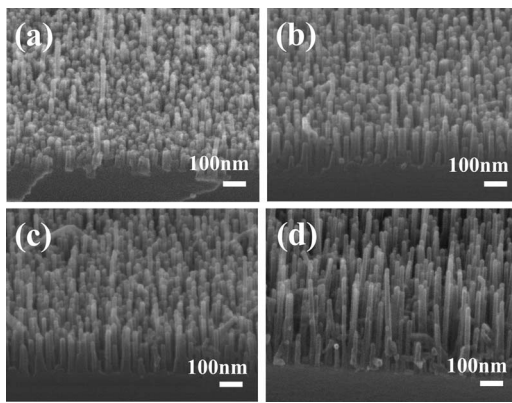


FIG. 1. FESEM images of MgO nanowires grown on MgO (100) single crystal substrate when varying the ambient oxygen pressure. The images are taken when the angle was tilted  $60^\circ$  to the substrate surface plane. The ambient oxygen pressures were (a) 0.01, (b) 0.1, (c) 1, and (d) 10 Pa.

ameter, the crystallinity, and the composition of the fabricated nanowires. Samples for HRTEM were prepared by placing a drop of the sample suspension on a copper microgrid (JEOL 7801-11613). HRTEM measurement was performed at the accelerating voltage of 300 kV.

Figure 1 shows the FESEM images of the MgO nanowires grown onto MgO (100) substrate when varying the ambient oxygen pressure. The nanowires were grown perpendicular to the substrate, indicating the (100) oriented epitaxial growth of the MgO nanowires. Although the size variation of diameter was relatively small, the significant dependence of the ambient oxygen pressure on the nanowire length was clearly observed. Figure 2(a) shows the effect of ambient oxygen pressure on the lengths of nanowires grown for 90 min. Figure 2(b) shows the variation of the length distribution data of nanowires grown under oxygen atmosphere when varying the ambient pressure. Clearly increasing the ambient oxygen pressure enhances the nanowire

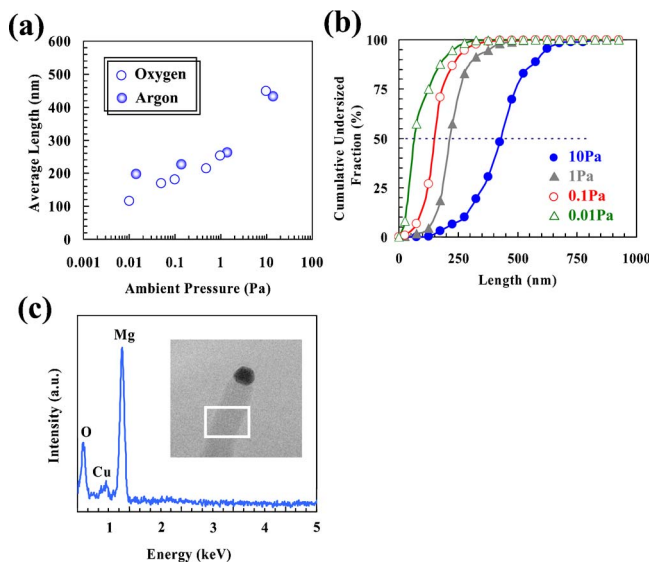


FIG. 2. (Color online) Ambient pressure dependence on the length of MgO nanowires under oxygen and/or argon atmospheres. Each sample was deposited for 90 min. (a) The opened circles show the data for nanowires grown under oxygen atmosphere, and the closed circles represent the data under argon atmosphere. (b) Length distribution data of nanowires grown under oxygen atmosphere are shown. (c) Shows the EDS data of nanowires grown under 10 Pa of argon atmosphere.

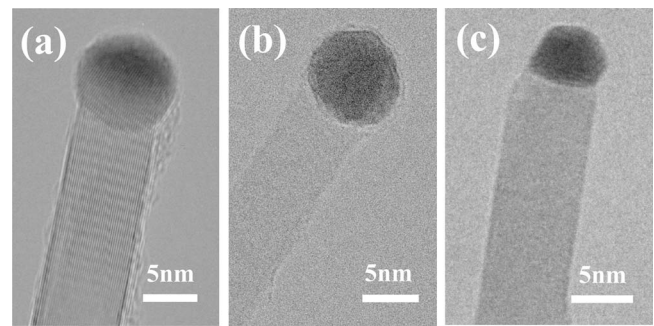


FIG. 3. HRTEM images of MgO nanowires. (a) and (b) show the images of nanowires grown under oxygen atmosphere with the ambient pressures of (a) 10 and (b) 0.01 Pa, respectively. Image (c) is of nanowire grown under argon atmosphere with the ambient pressures of 10 Pa.

growth. Since MgO nanowires contain oxygen, the incorporation of ambient oxygen from the surroundings into the oxide nanowires must occur during the nanowire growth. As such it is crucial to understand either such oxygen incorporation effect or the ambient pressure effect is dominant on the oxide nanowire growth. To distinguish such two effects, MgO nanowires were grown under argon atmosphere with varying the ambient pressure, and the results are shown in Fig. 2(a). Surprisingly it can be seen that the ambient pressure dependence on the nanowire length under argon atmosphere is exactly consistent with the trend under oxygen atmosphere. The presence of oxygen within MgO nanowires grown under argon atmosphere was confirmed by HRTEM-EDS analysis, as shown in Fig. 2(c). Note that oxygen under argon atmosphere must be supplied from the MgO single crystal target and/or residual oxygen in the chamber. In fact under lower background pressure ( $10^{-5}$  Pa), the degradation of MgO nanowire morphology deposited under argon atmosphere was observed, indicating that the presence of residual oxygen affects the MgO nanowire growth. However, it should be emphasized that increasing the ambient pressure much more strongly enhances the oxide nanowire growth even under argon atmosphere. Thus the enhancement of nanowire growth observed in Fig. 2 is mainly due to the ambient pressure effect rather than the amount of ambient oxygen. Figure 3 shows the typical HRTEM images of the near-tip MgO nanowires grown at (a) 10 and (b) 0.01 Pa under oxygen atmosphere, and (c) 10 Pa under argon atmosphere. As shown in Fig. 3(a), the clear lattice fringes were observed for the MgO nanowires fabricated under 10 Pa of the oxygen pressure, indicating the high crystallinity. It reveals that the spacing of 0.21 nm between the adjacent lattice planes corresponds to the distance between (200) crystal planes of MgO. Contrary, such lattice fringes were no longer observable for Figs. 3(b) and 3(c). These results highlight that the amount of ambient oxygen during oxide nanowire growth affects the crystallinity via the oxygen incorporation into nanowires rather than the nanowire morphology.

Here we assume the VLS mechanism for the MgO nanowire growth since the catalyst droplet was found on the tip of wires in the HRTEM image (Fig. 3). Recent intensive investigations in Si nanowire growth have revealed the significant role of the ambient oxygen on the growth.<sup>7</sup> Particularly, it was discovered that the presence of the ambient oxygen allows growing untapered and longer nanowires.<sup>7</sup> This is because the ambient oxygen reduces the Au diffusion along the sidewall of the nanowire away from the catalyst droplets,

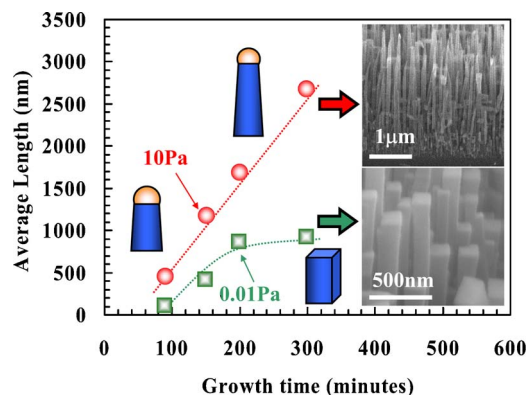


FIG. 4. (Color online) Time dependences on the nanowire length under different ambient oxygen pressures. Green squares show the data with the ambient pressure of 0.01 Pa, and the red circles are the data with the ambient pressure of 10 Pa. Inset: lower FESEM image shows the morphologies of nanowires grown for 300 min with the ambient pressure of 0.01 Pa, showing the disappearance of catalyst droplet and the sidewall growth. The upper FESEM image displays the nanowire morphologies grown for 300 min with the ambient pressure of 10 Pa, showing long nanowires up to 3–4  $\mu\text{m}$ .

which permits the droplet volumes to remain constant for longer time.<sup>7</sup> The other alternative interpretation is that the molecules adsorbed onto the droplet suppress the diffusion of the Au droplet, which is irrelevant to the vapor-liquid process at the droplet surface.<sup>6</sup> It should be noted that the effect of ambient oxygen on the oxide nanowire growth essentially differs from that of the Si nanowire growth<sup>7</sup> due to the oxygen incorporation into oxide nanowires. However, as shown in Fig. 2, the ambient pressure rather than the amount of ambient oxygen was found to critically enhance the MgO nanowire growth, indicating that surprisingly the same scenario as to the ambient oxygen effect on Si nanowire growth is applicable to the case of the oxide nanowire growth. That is, the ambient pressure even under argon atmosphere mainly reduces the Au catalyst diffusion away from the tip, resulting in the longer MgO nanowires. Assuming the interpretation based on the suppression of catalyst diffusion with increasing the ambient pressure, the disappearance of droplets should give rise as the catalyst diffusion progresses.<sup>4</sup> Figure 4 shows the time dependences on the lengths of nanowires deposited under 0.01 and 10 Pa of the ambient oxygen pressure. In the condition of 0.01 Pa, the growth rate tended to decrease after around 200 min, and then approaching the limited constant length. In the inset FESEM images, the disappearance of droplets was observed. The nanowire morphology tends to be square rod shapes due to the sidewall growth since the crystal structure of MgO is a rocksalt. These results clearly indicate the occurrence of the catalyst diffusion from the tip of the droplets. On the other hand, the nanowires grown under 10 Pa of the ambient oxygen pressure grew up to 3–4  $\mu\text{m}$  in length for 300 min with keeping the wire morphology, as shown in the inset FESEM images. These results highlight that the suppression of the Au diffusion away from the catalyst droplet rather than the oxygen incorporation into the oxide nanowires dominates the MgO nanowire growth when varying the ambient pressure.

In summary, we have shown the crucial role of ambient pressure on MgO nanowire growth. There are two major roles of oxygen pressure on oxide nanowire growth, such as the controllability of oxide nanowire growth rate and the

enhancement of crystallinity. The higher the ambient oxygen pressures the longer the nanowire length. Since the similar growth enhancement was found even under argon atmosphere, the ambient pressure rather than the amount of ambient oxygen dominates the nanowire growth via suppressing the catalyst diffusion from the tip. On the other hand, the amount of ambient oxygen strongly affects the nanowire crystallinity via the oxygen incorporation from the surroundings into the nanowires. The higher the ambient oxygen pressures, the higher the crystallinity. Although in the case of Si nanowire growth the presence of the ambient oxygen might be somehow detrimental due to the surface oxidization, whereas in the case of the oxide nanowires controlling the ambient oxygen pressure results in only positive effects, including the enhancements of both nanowire growth and the crystallinity. These experimental findings as to the oxide nanowire growth should provide an excellent controllability for various functional oxide nanowires, the heterostructures, and their applications.

The authors would like to thank the Ministry of Education, Culture, Sports, Science and Technology of Japan for funding and supporting this project through the Center of Excellence (COE) program. The authors also acknowledge Kanai for constructive advice and T. Ishibashi for his invaluable technical support. One of the authors (K.N.) gratefully acknowledges Micron Technology for the scholarship.

- <sup>1</sup>A. M. Morales and C. M. Liber, *Science* **279**, 208 (1998).
- <sup>2</sup>R. S. Wagner and W. C. Ellis, *Appl. Phys. Lett.* **4**, 89 (1964).
- <sup>3</sup>R. S. Wagner and W. C. Ellis, *Trans. Metall. Soc. AIME* **233**, 1052 (1965).
- <sup>4</sup>J. B. Hannon, S. Kodambaka, F. M. Ross, and R. M. Tromp, *Nature (London)* **440**, 69 (2006).
- <sup>5</sup>S. Kodambaka, J. Tersoff, M. C. Reuter, and F. M. Ross, *Phys. Rev. Lett.* **96**, 096105 (2006).
- <sup>6</sup>L. Cao, B. Garipcan, J. S. Atchison, C. Ni, B. Nabet, and J. E. Spanier, *Nano Lett.* **6**, 1852 (2006).
- <sup>7</sup>S. Kodambaka, J. B. Hannon, R. M. Tromp, and F. M. Ross, *Nano Lett.* **6**, 1292 (2006).
- <sup>8</sup>M. Yan, E. Zhang, J. Widjaja, and R. P. H. Chang, *J. Appl. Phys.* **94**, 5240 (2003).
- <sup>9</sup>B. P. Zhang, N. T. Binh, K. Wakatsuki, Y. Segawa, Y. Yamada, N. Usami, M. Kawasaki, and H. Koinuma, *Appl. Phys. Lett.* **84**, 4098 (2004).
- <sup>10</sup>M. Lorenz, E. M. Kaidashev, A. Rahm, Th. Nobis, J. Lenzner, G. Wagner, D. Spemann, H. Hochmuth, and M. Grundmann, *Appl. Phys. Lett.* **86**, 143113 (2005).
- <sup>11</sup>J. H. Park, Y. J. Choi, and J. G. Park, *J. Cryst. Growth* **280**, 161 (2005).
- <sup>12</sup>K. Nagashima, T. Yanagida, H. Tanaka, and T. Kawai, *J. Appl. Phys.* **100**, 063714 (2006).
- <sup>13</sup>T. Yanagida, T. Kanki, B. Vilquin, H. Tanaka, and T. Kawai, *J. Appl. Phys.* **99**, 053908 (2006).
- <sup>14</sup>H. Tian, Y. Wang, D. Wang, J. Miao, J. Qi, H. L. W. Chan, and C. L. Choy, *Appl. Phys. Lett.* **89**, 142905 (2006).
- <sup>15</sup>M. Ishikawa, H. Tanaka, and T. Kawai, *Appl. Phys. Lett.* **86**, 222504 (2005).
- <sup>16</sup>M. I. Faley, S. B. Mi, A. Petraru, C. L. Jia, U. Poppe, and K. Urban, *Appl. Phys. Lett.* **89**, 082507 (2006).
- <sup>17</sup>B. Lei, C. Li, D. Zhang, S. Han, and C. Zhou, *J. Phys. Chem. B* **109**, 18799 (2005).
- <sup>18</sup>C. Li, B. Lei, Z. Luo, S. Han, Z. Liu, D. Zhang, and C. Zhou, *Adv. Mater. (Weinheim, Ger.)* **17**, 1548 (2005).
- <sup>19</sup>K. Nagashima, T. Yanagida, H. Tanaka, and T. Kawai, *J. Appl. Phys.* **101**, 124304 (2007).
- <sup>20</sup>K. Nagashima, T. Yanagida, H. Tanaka, and T. Kawai, *Appl. Phys. Lett.* **90**, 233103 (2007).
- <sup>21</sup>A. Marcu, T. Yanagida, K. Nagashima, H. Tanaka, and T. Kawai, *J. Appl. Phys.* **102**, 016102 (2007).